Aerial-borne Data Management Center (ADMC)

Chieh Tsai, Hossein Rastgoftar, Salim Hariri
Department of Electrical and Computer Engineering
University of Arizona
Tucson, AZ 85719, USA
{vegetableclan, hrastgoftar, hariri}@arizona.edu

Abstract

Crisis management (CM) for critical infrastructures, natural disasters such as wildfires and hurricanes, terrorist actions, or civil unrest requires high-speed communications and connectivity, and access to high-performance computational resources to deliver timely dynamic responses to the crisis being managed by different first responders. CM systems should detect, recognize, and disseminate huge amounts of heterogeneous dynamic events that operate at different speeds and formats. Furthermore, the processing of crisis events and the development of real-time responses are major research challenges when the communications and computational resources needed by CM stakeholders are not available or severely degraded by the crisis. The main goal of the research presented in this paper is to utilize Unmanned Autonomous Systems (UAS) to provide an Aerial-borne Data Management Center (ADMC) that will provide the required communications services and the computational resources that are critically needed by first responders. In our approach to develop an ADMC architecture, we utilize a set of flexible Unmanned Aerial Systems (UAS) that can be dynamically composed to meet the communications and computational requirements of CM tasks. The ADMC services will be modeled as a deep neural network (DNN) mass transport approach to cover a distributed target in a decentralized manner. Furthermore, our analysis proves the stability and convergence of the proposed DNN-based mass transport for a team of UAS (e.g., quadcopters), where each quadcopter uses a feedback nonlinear control to independently attain the intended coverage trajectory in a decentralized manner.

1 Introduction

Over the past two decades, we have seen huge advancements in artificial intelligence and machine learning (AI/ML), mobile computing, cloud platforms, and Unmanned Aerial Systems (UAS) technologies. However, traditional information technology (IT) architectures are not properly equipped to utilize aerial and unmanned autonomous systems to provide agile communication and computation infrastructures that can keep pace with rapidly evolving application demands. This limitation becomes particularly critical in managing natural and malicious disasters, where IT infrastructures often become unavailable or severely degraded, rendering them ineffective for supporting crisis management (CM) tasks. CM applications share key characteristics such as mobility, dynamic behavior, nonlinear scaling, and sometimes unpredictable growth, depending on the size and nature of the inputs being processed.

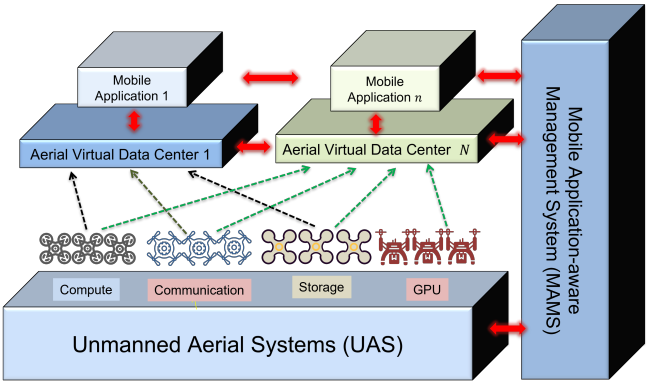

Figure 1: The proposed architecture for an Aerial-borne Data Management Center (ADMC) for simultaneous provision of computation resources for n applications, defined by $\mathcal{A} = \{1, \cdots, n\}$, using N Aerial Virtual Data Centers (AVDCs), defined by $\mathcal{V} = \{1, \cdots, N\}$.

The Service Level Objectives (SLOs) of CM applications are highly dynamic and unpredictable, necessitating continual provisioning and re-provisioning of communication and computational resources. Satisfying CM task requirements therefore represents major research challenges, especially when the communication and computational resources required by CM applications are unavailable or severely degraded by the crisis.

This paper aims to develop an innovative Aerial-borne Data Management Center (ADMC) architecture that utilizes a set of flexible Unmanned Aerial Systems (UAS) which can be dynamically and automatically assembled and reassembled to adapt to changing CM application demands (see Fig. 1). To this end, we develop aerial-borne architectural support, algorithms, and modeling techniques to enable the realization of composable data management centers that can efficiently and effectively respond to the evolving requirements of mobile, data-driven CM applications.

As shown in Fig. 1, we offer a mobile applicationaware management system (MAMS) that is aware of both the CM application characteristics and the underlying UAS infrastructures to break the barriers between CM applications, middleware/operating system, and UAS hardware layers. The vertical integration of these layers will enable us to build a dynamically customizable Aerial Virtual Data Center (AVDC) that will be optimized to meet the mobile CM application requirements such as QoS, availability, resilience, and energy. Our approach to develop the proposed ADMC architecture is shown in Fig. 1 that benefits from virtualization techniques in a variety of ways. Virtual Machines (VMs) have been widely used to provide a layer that is well-positioned in the hardware/software stack of computer systems. This provides fine-grain resource monitoring and control capabilities. In the ADMC approach, we scale the virtualization concept from being at the VM level to an Aerial Virtual Data Center (AVDC) level. For a given mobile application class, the ADMC middleware can build an AVDC that can meet the CM application Service Level Objectives (SLO) such as security, performance, energy consumption, resilience, or availability objectives. The selected AVDC will be then mapped into a set of available UAS resources that will provide the required computations, storage, and communications requirements. The composable UAS building blocks include heterogeneous drones that provide general purpose graphics processing units (GPUs), general purpose processors, storage capabilities and communications services.

1.1 Related Work

Traditional centralized data centers, while powerful, often struggle to meet emerging requirements for agility, geographic flexibility, and responsiveness. To address these limitations, researchers and industry practitioners have explored new paradigms such as mobile data centers, modular/adaptive data centers, and more recently, aerial and drone based computing platforms.

Mobile data centers—typically housed in ISO containers or portable enclosures—provide rapidly deployable computing capabilities for disaster response, military missions, remote industrial sites, and bandwidth constrained edge environments. (ENCOR Advisors 2025)

Building on these trends, the research community has increasingly investigated aerial mobile edge computing (MEC) systems, where unmanned aerial vehicles (UAVs) serve as airborne compute, communication, or sensing platforms. Comprehensive surveys describe how UAV enabled aerial MEC provides on demand computing resources, dynamic coverage, and improved service quality for latency sensitive IoT applications. Prior work explores challenges such as computation offloading, UAV trajectory optimization, resource allocation, scheduling, and the integration of AI driven optimization strategies.

Beyond serving as communication relays, drones are now envisioned as flying data centers capable of performing real time data processing at the extreme edge. Prototypes demonstrate drones equipped with miniaturized cloud stacks—using hyperconverged infrastructure—to perform localized analytics for applications including agriculture, transportation, and search and rescue. These systems reduce reliance on centralized cloud services by enabling ultra low latency machine to machine communication and distributed processing in the air. (Himairi 2025)

Aerial platforms have also become increasingly important in supporting ground based data centers through autonomous drone security and inspection systems. These systems offer improved coverage, faster reaction time, and reduced operational costs. (Adaptive MDC Ltd 2026)

Collectively, these developments demonstrate a growing convergence between mobile, modular, and aerial computing infrastructures. This work builds upon the above advancements to investigate the architectural, operational, and research opportunities that arise when mobile and aerial data center concepts are integrated to build Aerial-borne Data Management Center (ADMC).

ADMC considers UAS as Aerial Virtual Data Centers (AVDCs) that must be optimally and safely configured to provide the best internet coverage over specified areas on the ground. Our proposed method can be considered as a distributed coverage or mass transport problem, which has received significant attention in the control community. We propose a novel application of multi-agent coverage and mass transport problems to airborne communication infrastructure, whereas prior work has focused on different operational contexts.

Multi-agent coverage has found applications in wildfire management (Seraj, Silva, and Gombolay 2022; Haksar, Trimpe, and Schwager 2020; Gomez et al. 2015), border security (Pan et al. 2022), and agriculture (Din et al. 2022; Marwah et al. 2023). Related decentralized coverage formulations with finite-state or learning-based policies have also been studied for ground coverage and distributed target monitoring (Rastgoftar 2026, 2025).

Mass transport has garnered broad interest across diverse domains, including brain morphology (Gerber et al. 2023; Ma et al. 2019), image processing (Shakib et al. 2020; Song, Gu, and Kumar 2023), inverse problems (Stuart and Wolfram 2020), and cancer detection (Lin et al. 2021; Wang et al. 2010). Recent work has further explored aerial transport and coordination under cooperative and uncooperative agent interactions using deep learning–based methods (Zahed and Rastgoftar 2025).

Voronoi-based multi-agent coverage (Bai et al. 2021) has been widely investigated by the control community for uncovering distributed targets. In (Atınç, Stipanović, and Voulgaris 2020, 2014), Voronoi-based coverage is formulated as leader–follower and supervised control problems, where leaders identify regions of interest and followers perform coverage tasks. In (Chen, Georgiou, and Pavon 2016), the authors study the mass transport of linear systems from an initial configuration to an arbitrary target configuration and formulate it as an optimization problem with energy minimization objectives. Furthermore, mass transport has been cast within a linear quadratic Gaussian (LQG) regulation framework in (Hudoba de Badyn et al. 2021).

1.2 Contributions

The main contributions of this paper are summarized as follows:

- **Contribution 1: Unified architectural framework for mobile and aerial data centers.** We introduce a comprehensive ADMC architecture that unifies traditional portable containerized data centers, adaptive modular data center designs, and emerging UAV-based computing platforms. This framework clarifies how heterogeneous mobile and aerial infrastructures can operate cohesively to support scalable edge and near-edge computing services.
- **Contribution 2: On-demand aerial data management services under infrastructure degradation.** We develop an aerial-borne data management paradigm that provides on-demand and real-time communication services and computational resources for target areas where IT infrastructures are unavailable or severely degraded due to natural or malicious disasters (e.g., wildfires, earthquakes, hurricanes).
- **Contribution 3: DNN-based inter-AVDC communication and configuration modeling.** We employ a DNN to define inter-AVDC communications, where the DNN structure accurately represents the reference configuration of the AVDC team. The reference configuration and the corresponding DNN structure are dynamically updated whenever the number of AVDCs changes, accommodating the limited mission duration and dynamic availability of aerial assets.
- **Contribution 4: Forward training method for fast and stable convergence.** We propose a novel *forward* training method for the DNN that enables fast convergence, in contrast to conventional neural network training approaches that do not necessarily guarantee convergence.
- **Contribution 5: Decentralized multi-AVDC coordination with stability guarantees.** We formulate the AVDC-based internet service provision problem as a decentralized multi-AVDC coordination problem with time-varying weights. By modeling each AVDC as a multi-copter drone, we guarantee inter-AVDC stability using a nonlinear dynamic model recently developed in (El Asslouj and Rastgoftar 2023).

This paper is organized as follows. Section 2 provides a solution for determining the DNN structure based on the AVDC reference configuration. Our proposed forward method for training the DNN is presented in Section 4. We define the data service provision problem as a decentralized multi-AVDC coordination with time-varying weights in Section 5. Simulation results are presented in Section 6, followed by concluding remarks in Section 7.

2 Problem Statement

The proposed ADMC architecture requires a mathematical formulation to enable the real-time management of the operational requirements of the AVDCs such that they can provide the required aerial computation and communication services over geographically distributed crisis zones. We consider an aerial-borne data center environment to be consistent of N AVDCs operating above the ground, where the set $\mathcal{V} = \{1, \ldots, N\}$ identifies the AVDCs. The AVDCs are deployed to provide internet connectivity and computational services for distinct applications, defined by the set $\mathcal{A} = \{1, \ldots, n\}$. Each application $i \in \mathcal{A}$ is executed over a two-dimensional geographic domain consisting of multiple desirable target zones, each of which is geofenced by a ground-based polygon.

Each AVDC represents a mobile, resource-constrained aerial platform whose physical position directly determines both wireless coverage quality and computational service availability. Consequently, the collective behavior of the AVDC team must continuously adapt to spatially heterogeneous and time-varying service demands induced by crisis response applications. To capture this interaction in a principled and scalable manner, we model the AVDC team as a graph-structured, DNN-equivalent system. This representation enables explicit encoding of inter-AVDC communication, coordination, and hierarchy in a form that is compatible with decentralized control and dynamic reconfiguration.

Within this framework, the provision of services is modeled as a mass-transport problem, where application demand over the ground induces a spatial redistribution of AVDCs through continuous deformation of their formation. Communication weights act as physically meaningful influence coefficients that determine how local AVDC interactions collectively realize global coverage objectives. At the same time, the nonlinear multi-copter dynamics governing each AVDC ensure that the resulting service allocation and reconfiguration remain dynamically feasible. As a result, the proposed formulation establishes a direct bridge between abstract coordination laws and the practical requirements of resilient, on-demand aerial crisis management infrastructure.

We define the joint provision of communication and computational services as a *decentralized multi-agent coordination problem* over a finite time horizon with time-varying communication weights. The objective is to ensure safe, scalable, and adaptive service provision starting from an arbitrary initial AVDC configuration and converging to a desired target configuration dictated by application demand. To this end, the problem is decomposed into the following three sub-problems.

Problem 1 (Communication Structure): Determine a directed communication graph $\mathcal{G}(\mathcal{V}, \mathcal{E})$ among the AVDCs, where $\mathcal{E} \subseteq \mathcal{V} \times \mathcal{V}$ defines inter-AVDC communication links, such that the resulting graph admits a deep neural network (DNN) representation. The communication structure must support decentralized coordination, scalability with the number of AVDCs, and safe convergence from arbitrary initial formations to desired coverage configurations.

Problem 2 (Communication Weights): Given the communication structure, determine initial, final, and time-varying communication weights that are consistent with AVDC configurations and reflect the spatial distribution and priorities of ground applications. The communication weights must enable smooth, stable, and collision-free reconfiguration of the AVDC team from the initial configuration to the desired target configuration.

Problem 3 (Decentralized Service Provision): Assuming each AVDC is modeled as a multi-copter UAS with nonlinear dynamics, design decentralized control laws that use the time-varying communication weights to ensure dynamically feasible motion and convergence of the AVDC team to the desired service-provision configuration.

3 Inter-AVDC Communication Structure

This section translates the ADMC architectural requirement for scalable AVDC reconfiguration into an analytical formulation by constructing a DNN-convertible inter-AVDC communication graph that supports decentralized CM service provision. To ensure that graph $\mathcal{G}(\mathcal{V}, \mathcal{E})$, defining fixed inter-AVDC communication links, can be converted to a deep neural network, we first divide $\mathcal{V}$ into $M+1$ disjoint subsets that are denoted by $\mathcal{V}_0$, $\mathcal{V}_1$, $\cdots$, $\mathcal{V}_M$, i.e. $\mathcal{V}$ can be expressed as $\mathcal{V} = \bigcup_{l\in\mathcal{M}} \mathcal{V}_l$. We can also express set $\mathcal{V}$ as

$$\mathcal{V} = \bigcup_{l\in\mathcal{M}} \mathcal{W}_l, \tag{1}$$

where $\mathcal{W}_l$ is related to $\mathcal{V}_l$ by

$$\mathcal{W}_l = \begin{cases} \mathcal{V}_l & l \in \{0, M\} \\ \mathcal{V}_l \cup \mathcal{W}_{l-1} & l \in \mathcal{M}\setminus\{0, M\} \end{cases}. \tag{2}$$

We then define in-neighbors of every AVDC $i \in \mathcal{V}_l$ by finite set $\mathcal{N}_i$ such that the following condition holds:

$$\bigwedge_{l\in\mathcal{M}\setminus\{0\}} \bigwedge_{i\in\mathcal{V}_l} (\mathcal{N}_i \subset \mathcal{W}_{l-1}), \tag{3}$$

Given $\mathcal{N}_i$, we define

$$\mathcal{I}_{i,l} = \begin{cases} \mathcal{N}_i & i \in \mathcal{V}_l \\ \{i\} & i \in \mathcal{W}_l \setminus \mathcal{V}_l \end{cases}, \qquad \forall l \in \mathcal{M}\setminus\{0\}, \tag{4}$$

as the set of neurons connected to $i \in \mathcal{W}_l$, from layer $l-1 \in \mathcal{M}$.

Set $\mathcal{V}_0$: Given reference positions of the AVDCs, set $\mathcal{V}$ can be expressed as $\mathcal{V} = \mathcal{V}_B \cup \mathcal{V}_I$, where $\mathcal{V}_B$ and $\mathcal{V}_I$ are disjoint subsets of $\mathcal{V}$ defining "boundary" and "interior" AVDCs , respectively. *In this work, we assume that the AVDC team are contained by a convex polytope whose vertices are occupied by the boundary AVDCs.*

Given the reference configuration of the AVDC team, we also determine the core leader AVDC. Core leader is an interior AVDC that is at the closest distance from the boundary AVDCs, and assigned by solving the following optimization problem:

$$c(\mathcal{V}_B) = \underset{j\in\mathcal{V}_I}{\operatorname{argmin}} \left(\sum_{h\in\mathcal{V}_B} \|\mathbf{a}_h - \mathbf{a}_j\| \right). \tag{5}$$

where $\mathbf{a}_i$ is the reference (initial) position of agent $i \in \mathcal{V}$. Set

$$\mathcal{V}_0 = \mathcal{V}_B \bigcup c(\mathcal{V}_B) \tag{6}$$

includes the boundary and core AVDCs. Note that $\mathcal{V}_0$'s AVDCs are called leaders because they do not communicate with any other AVDCs to evolve in the motion space. This property of $\mathcal{V}_0$ can be formally specified by

$$\bigwedge_{i\in\mathcal{V}_0} (\mathcal{N}_i = \emptyset). \tag{7}$$

Sets $\mathcal{V}_1$ through $\mathcal{V}_{M-1}$: AVDCs defined by $\mathcal{V}_l$, for every $l \in \mathcal{M}\setminus\{0, M\}$ can act as both followers and in-neighbors. More specifically, $\mathcal{V}_l$'s AVDCs act as followers because their in-neighbors are subsets of $\mathcal{V}_{l-1}$. On the other hand, every AVDC $i \in \mathcal{V}_l$ is an in-neighbor for at least one AVDC belonging to $\mathcal{V}_{l+1}$, when $l \in \mathcal{M}\setminus\{0, M\}$.

Set $\mathcal{V}_M$: The AVDC defined by $\mathcal{V}_M$ are pure followers which mean that $\mathcal{V}_M$'s AVDCs update their own positions based on positions of ther in-neighbors, belonging to $\mathcal{V}_{M-1}$, but, they do not act as in-neighbors for any other AVDCs.

We desire that the reference communication weights are unique and consistent with the AVDC's positions. To this end, we restrict inter-AVDC communication to satisfy the following two requirements:

Requirement 1: Every AVDC $i \in \mathcal{V}\setminus\mathcal{V}_0$ solely communicates with three AVDCs. Therefore,

$$\bigwedge_{l\in\mathcal{M}\setminus\{0\}} \bigwedge_{i\in\mathcal{V}_l} (|\mathcal{N}_i| = 3), \tag{8}$$

To be more precise, in-neighbors of $i \in \mathcal{V}\setminus\mathcal{V}_0$ are placed at vertices of a triangle that encloses $i \in \mathcal{V}\setminus\mathcal{V}_0$. This triangle, is called the *communication triangle* of AVDC $i \in \mathcal{V}\setminus\mathcal{V}_0$.

Requirement 2: If this requirement is satisfied, reference communication weight $\omega_{i,j}$, between AVDC $i \in \mathcal{V}\setminus\mathcal{V}_0$ and $j \in \mathcal{N}_i$, is unique, positive, consistent with reference configuration, and obtained by solving the following equations:

$$\mathbf{a}_i = \sum_{j\in\mathcal{N}_i} \omega_{i,j}\mathbf{a}_j, \qquad \forall i \in \mathcal{V}, \tag{9a}$$

$$\sum_{j\in\mathcal{N}_i} \omega_{i,j} = 1, \qquad \forall i \in \mathcal{V}, \tag{9b}$$

4 Forward Method for Training the DNN

This section formalizes how CM-driven service demand is incorporated into the ADMC control framework by mapping the CM service distribution, represented by a heat map, into desired AVDC positions and time-varying communication weights within the DNN. To train the DNN, we first generate a heat map to specify the target distribution by a continuous and differentiable field over a two-dimensional motion space. By knowing the heat map and the DNN structure, we develop a mass-centric approach to update the desired final position of every AVDC. Lastly, we formulate DNN weights based AVDCs' desired positions in Section 4.3.

4.1 Service Distribution Heat Map

For service application $j \in \mathcal{A}$, we let set $\mathcal{D}_j$ define discrete target points where $\mathbf{d}_{i,j}$ denotes the position of target $i \in \mathcal{D}_j$, for $j \in \mathcal{A}$. Then, we define heat map $\mathcal{H}_j : \mathbb{R}^2 \to \mathbb{R}_+$ for $j \in \mathcal{A}$ by the following multi-variate Gaussian distribution:

$$\mathcal{H}_j(\mathbf{r}, \mathcal{D}_j) = \frac{1}{|\mathcal{D}_j|}(2\pi)^{-1} \sum_{i\in\mathcal{D}_j} \det(\mathbf{\Sigma}_i)^{\frac{-1}{2}} \exp\left(-(\mathbf{r}-\mathbf{d}_{i,j})^T \mathbf{\Sigma}_i^{-1}(\mathbf{r}-\mathbf{d}_{i,j})^T\right), \tag{10}$$

where $\mathbf{\Sigma}_i$ is the covariance matrix corresponding to target $i \in \mathcal{D}_j$; $\alpha_j \in [0,1]$ is a positive weight to quantify the priority of application $j \in \mathcal{A}$, where

$$\sum_{j \in \mathcal{A}} \alpha_j = 1. \tag{11}$$

The service distribution heat map (SDHM) is defined by

$$\mathcal{H}(\mathbf{r}) = \sum_{j \in \mathcal{A}} \alpha_j \mathcal{H}_j(\mathbf{r}, \mathcal{D}_j). \tag{12}$$

4.2 AVDCs' Desired Positions

Given the target set distribution, we determine the (final) desired position of every AVDC $i \in \mathcal{V}$ so that the best coverage of the SDHM is achieved. Desired position of the core AVDC is assigned based on the desired positions of the boundary AVDCs by

$$\mathbf{p}_{c(\mathcal{V}_B)} = \frac{\sum_{i \in \mathcal{V}_B} \mathbf{p}_i}{|\mathcal{V}_B|}. \tag{13}$$

Therefore, positions of $\mathcal{V}_0$'s AVDCs are known and constant at any time t. By defining

$$\mathcal{C}_i = \left\{ \sum_{j \in \mathcal{N}_i} \gamma_j \mathbf{p}_j \subset \mathbb{R}^n : \sum_{j \in \mathcal{N}_i} \gamma_j = 1,\ \gamma_j \geq 0, \forall j \in \mathcal{N}_i \right\} \tag{14}$$

as the convex hull specified by the in-neighbors of AVDC $i \in \mathcal{V} \setminus \mathcal{V}_0$, desired position of every multi-copter $i \in \mathcal{V} \setminus \mathcal{V}_0$ is obtained by

$$\mathbf{p}_i = \frac{\int_{\mathcal{C}_i} \mathcal{H}(\mathbf{r})\, d\mathbf{r}}{\int_{\mathcal{C}_i} d\mathbf{r}}, \qquad i \in \mathcal{V} \setminus \mathcal{V}_0. \tag{15}$$

4.3 Communication Weights

In-neighbors of every multi-copter $i \in \mathcal{V}$, defined by $\mathcal{N}_i$, are at vertices of a triangle enclosing $i \in \mathcal{V}$. Because of this, we can express (final) desired position $\mathbf{p}_i$ as the convex combination of desired positions of its in-neighbors as follows:

$$\mathbf{p}_i = \sum_{j \in \mathcal{N}_i} \varpi_{i,j} \mathbf{p}_j, \qquad \forall i \in \mathcal{V}, \tag{16a}$$

$$\sum_{j \in \mathcal{N}_i} \varpi_{i,j} = 1, \qquad \forall i \in \mathcal{V}, \tag{16b}$$

where $\varpi_{i,j}$ is the final communication weight of $i \in \mathcal{V}$ with in-neighbor $j \in \mathcal{N}_i$. The communication weight of AVDC $i \in \mathcal{V}$ with $j \in \mathcal{N}_i$ is then denoted by $w_{i,j}(t)$ and defined as follows:

$$w_{i,j}(t) = \begin{cases} (1 - \beta(t))\, \omega_{i,j} + \beta(t) \varpi_{i,j} & t \in [0, t_f] \\ \varpi_{i,j} & t \geq t_f \end{cases}, \tag{17}$$

where t_0 and t_f denote the reference and final times, respectively; $\omega_{i,j}$ is the initial communication weights obtained by Eqs. (9a) and (9b); and $\beta : [0, t_f] \to [0,1]$ is an increasing function satisfying $\beta(t_0) = 0$ and $\beta(t_f) = 1$. The quintic scheduling profile used for $\beta(t)$ is shown in Fig. 5.

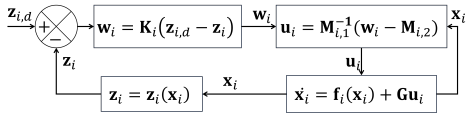

Figure 2: The block diagram of the trajectory tracking control used by every AVDC $i \in \mathcal{V}$.

5 Decentralized Internet Coverage

This section implements the ADMC analytical framework at the execution level by embedding the DNN-based coordination law into the nonlinear UAS dynamics, enabling each AVDC to follow the intended service trajectory in a decentralized manner. The internet coverage problem is defined as decentralized multi-agent coordination structured by the DNN, where the DNN's neurons are operated by differential equations. Particularly, neuron $i \in \mathcal{W}_l$ ($l \in \mathcal{M}$) represents AVDC $i \in \mathcal{V}$ where the dynamics of AVDC $i \in \mathcal{V}$ iven by

$$\begin{cases} \dot{\mathbf{x}}_i = \mathbf{F}_i(\mathbf{x}_i, \mathbf{u}_i) \\ \mathbf{r}_i = \mathbf{h}_i(\mathbf{x}_i) \end{cases} \tag{18}$$

operates neuron $i \in \mathcal{V}$. Note that $\mathbf{x}_i$ and $\mathbf{u}_i$ are the state and input vectors of dynamics (18), respectively, and $\mathbf{r}_i$ denoting position of AVDC $i \in \mathcal{V}$, is considered as the output vector of dynamics (18). The input vector of agent $i \in \mathcal{V}$ is defined by

$$\mathbf{r}_{i,d} = \begin{cases} \mathbf{p}_i & i \in \mathcal{V}_0 \\ w_{i,j} \mathbf{r}_j & i \in \mathcal{V} \setminus \mathcal{V}_0 \end{cases} \tag{19}$$

5.1 AVDC Motion Model

Assuming AVDC $i \in \mathcal{V}$ is a multi-copter UAS with mass m_i, we use the nonlinear dynamics presented in (Rastgoftar and Kolmanovsky 2021) to obtain $\mathbf{F}_i(\mathbf{x}_i, \mathbf{u}_i)$. The state vector $\mathbf{x}_i \in \mathbb{R}^{14 \times 1}$ is given by

$$\mathbf{x}_i = \begin{bmatrix} x_i\ y_i\ z_i\ \dot{x}_i\ \dot{y}_i\ \dot{z}_i\ \phi_i\ \theta_i\ \psi_i\ \dot{\phi}_i\ \dot{\theta}_i\ \dot{\psi}_i\ f_i\ \dot{f}_i \end{bmatrix}^T \tag{20}$$

where x_i, y_i, and z_i define UAS position components at (continuous) time t; ϕ_i, θ_i, and ψ_i define roll, pitch, and yaw angles of AVDC $i \in \mathcal{V}$; and f_i is the magnitude of the thrust force generated by AVDC $i \in \mathcal{V}$. We also define

$$\mathbf{u}_i = [u_{1,i}\ u_{2,i}\ u_{3,i}\ u_{4,i}]^T \tag{21}$$

where $u_{1,i} = \ddot{f}_i$, $u_{2,i} = \ddot{\phi}_i$, $u_{3,i} = \ddot{\theta}_i$, and $u_{4,i} = \ddot{\psi}_i$. We can express $\mathbf{F}_i(\mathbf{x}_i, \mathbf{u}_i)$ as

$$\mathbf{F}_i(\mathbf{x}_i, \mathbf{u}_i) = \mathbf{f}_i(\mathbf{x}_i) + \mathbf{G}\mathbf{u}_i, \tag{22}$$

where

$$\mathbf{f}_i(\mathbf{x}_i) = \begin{bmatrix} \dot{x}_i \\ \dot{y}_i \\ \dot{z}_i \\ \frac{f_i}{m_i}(\sin\phi_i \sin\psi_i + \cos\phi_i \cos\psi_i \sin\theta_i) \\ \frac{f_i}{m_i}(\cos\phi_i \sin\psi_i \sin\theta_i - \sin\phi_i \cos\psi_i) \\ \frac{f_i}{m_i}\cos\phi_i \cos\theta_i - g \\ \dot{\phi}_i \\ \dot{\theta}_i \\ \dot{\psi}_i \\ 0 \\ 0 \\ 0 \\ \dot{f}_i \\ 0 \end{bmatrix}, \quad \mathbf{G} = [\mathbf{g}_1 \quad \cdots \quad \mathbf{g}_4] = \begin{bmatrix} \mathbf{0}_{9\times1} & \mathbf{0}_{9\times3} \\ \mathbf{0}_{3\times1} & \mathbf{I}_3 \\ 0 & \mathbf{0}_{1\times3} \\ 1 & \mathbf{0}_{1\times3} \end{bmatrix}.$$

Note that $g = 9.81 m/s^2$ is the gravity acceleration.

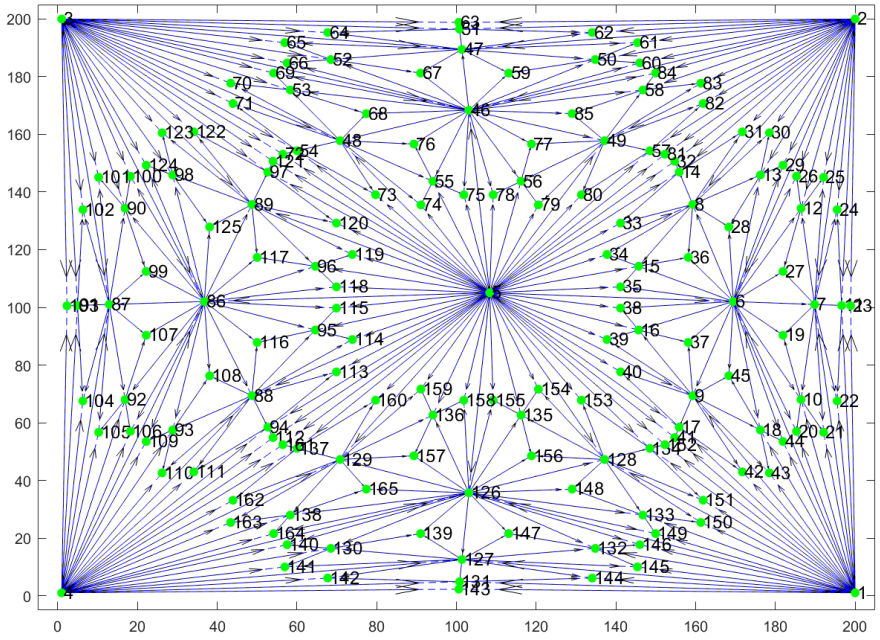

Figure 3: The initial formation of the AVDC team and inter-agent communication links.

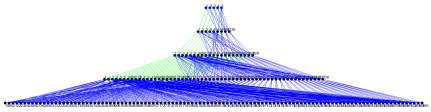

Figure 4: The structure of the DNN assigned based on the reference configuration of the AVDC team.

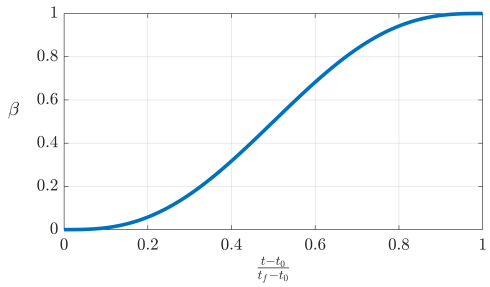

Figure 5: The quintic polynomial used for defining β versus $\frac{t-t_0}{t_f-t_0}$.

5.2 AVDC Trajectory Tracking

The objective of trajectory tracking is to choose $\mathbf{u}_i$ such that $\mathbf{r}_{i,d}$ stably tracks the desired input $\mathbf{r}_{i,d}$. By applying the feedback linearization method developed in Refs. (El Asslouj and Rastgoftar 2023; Rastgoftar and Kolmanovsky 2021), we define state transformation

$$\mathbf{z}_i\left(\mathbf{x}_i\right)=\begin{bmatrix}\mathbf{r}_i^T & \dot{\mathbf{r}}_i^T & \ddot{\mathbf{r}}_i^T & \dddot{\mathbf{r}}_i^T & \psi_i & \dot{\psi}_i\end{bmatrix}^T \tag{23}$$

and let $\mathbf{z}_i$ be updated by the following dynamics:

$$\dot{\mathbf{z}}=\mathbf{A}\mathbf{z}+\mathbf{B}\mathbf{w}_i, \tag{24}$$

where $\mathbf{w}_i=\begin{bmatrix}\dddot{x} & \dddot{y} & \dddot{z} & \ddot{\psi}\end{bmatrix}^T$ is the control input of external dynamics (24), and

$$\mathbf{A}=\begin{bmatrix}\mathbf{0}_{9\times3} & \mathbf{I}_9 & \mathbf{0}_{9\times1} & \mathbf{0}_{9\times1}\\ \mathbf{0}_{3\times3} & \mathbf{0}_{3\times9} & \mathbf{0}_{3\times1} & \mathbf{0}_{3\times1}\\ \mathbf{0}_{1\times3} & \mathbf{0}_{1\times9} & 0 & 1\\ \mathbf{0}_{1\times3} & \mathbf{0}_{1\times9} & 0 & 0\end{bmatrix} \tag{25}$$

$$\mathbf{B}=\begin{bmatrix}\mathbf{0}_{9\times3} & \mathbf{0}_{9\times1}\\ \mathbf{I}_3 & \mathbf{0}_{3\times1}\\ \mathbf{0}_{1\times3} & 0\\ \mathbf{0}_{1\times3} & 1\end{bmatrix} \tag{26}$$

Note that $\mathbf{w}_i$ is related to the control input of multi-copter UAS, denoted by $\mathbf{u}_i$, by

$$\mathbf{w}_i=\mathbf{M}_{i,1}\mathbf{u}_i+\mathbf{M}_{i,2}, \tag{27}$$

where

$$\mathbf{M}_{i,1}=\begin{bmatrix}L_{g_1}L_{f_i}^3x & L_{g_2}L_{f_i}^3x & L_{g_3}L_{f_i}^3x & L_{g_4}L_{f_i}^3x\\ L_{g_1}L_{f_i}^3y & L_{g_2}L_{f_i}^3y & L_{g_3}L_{f_i}^3y & L_{g_4}L_{f_i}^3y\\ L_{g_1}L_{f_i}^3z & L_{g_2}L_{f_i}^3z & L_{g_3}L_{f_i}^3z & L_{g_4}L_{f_i}^3z\\ L_{g_1}L_{f_i}\psi & L_{g_2}L_{f_i}\psi & L_{g_3}L_{f_i}\psi & L_{g_4}L_{f_i}\psi\end{bmatrix}\in\mathbb{R}^{4\times4} \tag{28a}$$

$$\mathbf{M}_{i,2}=\begin{bmatrix}L_{f_i}^4x & L_{f_i}^4y & L_{f_i}^4z & L_{f_i}^2\psi\end{bmatrix}^T\in\mathbb{R}^{4\times1} \tag{28b}$$

$$\mathbf{M}_{i,2}=\begin{bmatrix}L_{\mathbf{f}_i}^4x & L_{\mathbf{f}_i}^4y & L_{\mathbf{f}_i}^4z & L_{\mathbf{f}_i}^2\psi\end{bmatrix}^T\in\mathbb{R}^{4\times1}. \tag{29}$$

To achieve the control objective, we choose

$$\mathbf{w}_i=\mathbf{K}_i\left(\mathbf{z}_{i,d}-\mathbf{z}_i\right) \tag{29}$$

such that $\mathbf{z}_i$ stably tracks

$$\mathbf{z}_{i,d}=\begin{bmatrix}\mathbf{r}_{i,d}^T & \mathbf{0}_{1\times9} & \psi_d & 0\end{bmatrix}^T,$$

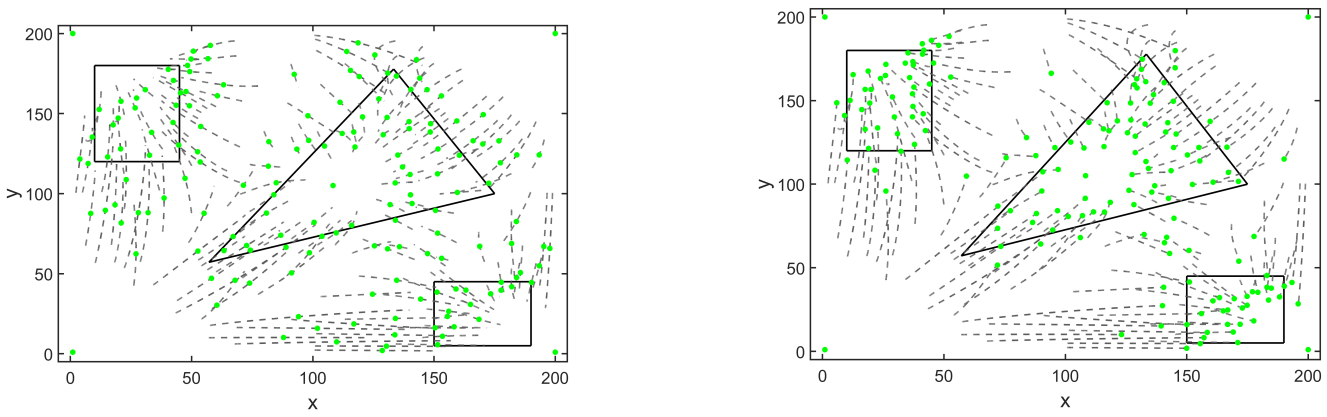

(a) $t = 35\,\mathrm{s}$ (b) $t = 80\,\mathrm{s}$

Figure 6: Formation evolution of the AVDC team at selected time instances.

where $\mathbf{r}_{i,d} \in \mathbb{R}^{3\times 1}$ given by Eq. (19) is the UAS desired trajectory, and $\psi_d = 0$ is the desired yaw angle of AVDC $i \in \mathcal{V}$. This control objective is achieved, if $\mathbf{A}-\mathbf{B}\mathbf{K}_i$ is Hurwitz, for every $i \in \mathcal{V}$. Then, the AVDC control is obtained by

$$\mathbf{u}_i = \mathbf{M}_{i,1}^{-1}\left(\mathbf{w}_i - \mathbf{M}_{i,2}\right). \tag{30}$$

Figure 2 shows the block diagram of the proposed control applied by every AVDC $i \in \mathcal{V}$. Proofs for the stability and convergence of the proposed trajectory tracking control were provided in (Rastgoftar, Atkins, and Kolmanovsky 2021; Rastgoftar and Kolmanovsky 2021; El Asslouj and Rastgoftar 2023).

6 Simulation Results

The simulations evaluate whether the proposed ADMC architecture satisfies CM task requirements by verifying that the DNN-based mass transport model yields stable, convergent, and decentralized AVDC reconfiguration under nonlinear UAS dynamics. We consider an AVDC team identified by set $\mathcal{V} = \{1, \cdots, 165\}$ with the reference configuration shown in Fig. 3. We desire that the AVDC team provides computation resources over the separated rectangular and triangular domains shown in Fig. 3. Given the reference formation, the inter-agent communication is obtained and graphically shown in Fig. 3. This inter-AVDC communication links can be represented by the deep neural network shown in Fig. 4.

By knowing the DNN structure, the initial communication weight and final desired position of every AVDC are obtained by using the approach presented in Section 4.2. The desired configuration of the AVDCs is shown by points in Fig. 3. By knowing the final desired positions of the agents, the final communication weights are obtained by (16) and the transient communication weigh is defined for every agent $i \in \mathcal{V}$ using Eq. (17) over the time interval $[0, 60s]$, where $\beta(t)$ is defined by a quintic polynomial and plotted in Fig. 5.

To implement the proposed coverage approach, we assume every agent is a quadcopter UAS and apply the quadcopter model and trajectory tracking control developed in (El Asslouj and Rastgoftar 2023; Rastgoftar and Kolmanovsky 2021) to operate DNN neurons. Figure 6 presents the formation evolution snapshots at $t = 35\,\mathrm{s}$ and $t = 80\,\mathrm{s}$, where the actual path of every AVDC $i \in \mathcal{V}$, from $\mathbf{a}_i$ to $\mathbf{p}_i$, is shown by dashed red.

6.1 Limitations and Practical Considerations

Despite its adaptability under nonlinear dynamics, the ADMC framework may incur computational and communication overhead in large-scale deployments. In addition, uncertainty in demand estimation during crisis scenarios may affect resource allocation performance.

7 Conclusion

In summary, this work links ADMC requirements for CM tasks to a provable framework using DNN-based mass transport with time-varying weights and decentralized nonlinear UAS dynamics. Our research approach will utilize mobile application-aware management system (MAMS) that is aware of both the application characteristics and the underlying UAS infrastructures to break the barriers between applications, middleware/operating system, and UAS hardware layers. The vertical integration of these layers will enable us to build a dynamically customizable Aerial Virtual Data Center (AVDC) that will be optimized to meet the mobile application requirements such as QoS, availability, resilience, and energy. Our approach to develop the proposed Aerial-based Mobile Composable Data center (AMCDC) is shown in Figure 1 that benefits from virtualization techniques in a variety of ways. Virtual Machines (VMs) have been widely used to provide a layer that is well-positioned in the hardware/software stack of computer systems. This provides fine-grain resource monitoring and control capabilities. In the AMCDC approach, we scale the virtualization concept from being at the VM level to an Aerial Virtual Data Center (AVDC) level. For a given mobile application class, the AMCDC middleware can build a AVDC that can meet the application Service Level Objectives (SLO) such

as security, performance, energy consumption, resilience, or availability objectives. The selected AVDC will be then mapped into a set of available UAS resources that will provide the required computation, storage, communications requirements. The composable UAS building blocks include heterogeneous drones that provide general purpose graphics processing units (GPUs), general purpose processors, storage capabilities and communications services.

References

Adaptive MDC Ltd. 2026. Adaptive MDC – Build the Future Today. https://www.adaptive-mdc.com/. Accessed: 2026-02-07.

Atınç, G. M.; Stipanović, D. M.; and Voulgaris, P. G. 2014. Supervised coverage control of multi-agent systems. *Automatica*, 50(11): 2936–2942.

Atınç, G. M.; Stipanović, D. M.; and Voulgaris, P. G. 2020. A swarm-based approach to dynamic coverage control of multi-agent systems. *Automatica*, 112: 108637.

Bai, Y.; Wang, Y.; Svinin, M.; Magid, E.; and Sun, R. 2021. Adaptive multi-agent coverage control with obstacle avoidance. *IEEE Control Systems Letters*, 6: 944–949.

Chen, Y.; Georgiou, T. T.; and Pavon, M. 2016. Optimal transport over a linear dynamical system. *IEEE Transactions on Automatic Control*, 62(5): 2137–2152.

Din, A.; Ismail, M. Y.; Shah, B.; Babar, M.; Ali, F.; and Baig, S. U. 2022. A deep reinforcement learning-based multi-agent area coverage control for smart agriculture. *Computers and Electrical Engineering*, 101: 108089.

El Asslouj, A.; and Rastgoftar, H. 2023. Quadcopter tracking using euler-angle-free flatness-based control. In *2023 European Control Conference (ECC)*, 1–6. IEEE.

ENCOR Advisors. 2025. The Modular Data Center Ultimate Guide. https://encoradvisors.com/modular-data-center/. Accessed: 2026-02-07.

Gerber, S.; Niethammer, M.; Ebrahim, E.; Piven, J.; Dager, S. R.; Styner, M.; Aylward, S.; and Enquobahrie, A. 2023. Optimal transport features for morphometric population analysis. *Medical Image Analysis*, 84: 102696.

Gomez, M.; Kim, Y.; Matson, E.; Tolstykh, M.; and Munizzi, M. 2015. Multi-agent system of systems to monitor wildfires. In *2015 10th System of Systems Engineering Conference (SoSE)*, 262–267. IEEE.

Haksar, R. N.; Trimpe, S.; and Schwager, M. 2020. Spatial scheduling of informative meetings for multi-agent persistent coverage. *IEEE Robotics and Automation Letters*, 5(2): 3027–3034.

Himairi, H. 2025. Data Center Adaptive Reuse: 5 Strategies for Existing Buildings. https://www.dlrgroup.com/idea/data-center-adaptive-reuse-strategies/. Published April 10, 2025; Accessed: 2026-02-07.

Hudoba de Badyn, M.; Miehling, E.; Janak, D.; Açıkmeşe, B.; Mesbahi, M.; Başar, T.; Lygeros, J.; and Smith, R. S. 2021. Discrete-Time Linear-Quadratic Regulation via Optimal Transport. *arXiv e-prints*, arXiv–2109.

Lin, W.-W.; Juang, C.; Yueh, M.-H.; Huang, T.-M.; Li, T.; Wang, S.; and Yau, S.-T. 2021. 3D brain tumor segmentation using a two-stage optimal mass transport algorithm. *Scientific reports*, 11(1): 14686.

Ma, M.; Wang, X.; Duan, Y.; Frey, S. H.; and Gu, X. 2019. Optimal mass transport based brain morphometry for patients with congenital hand deformities. *The Visual Computer*, 35: 1311–1325.

Marwah, N.; Singh, V. K.; Kashyap, G. S.; and Wazir, S. 2023. An analysis of the robustness of UAV agriculture field coverage using multi-agent reinforcement learning. *International Journal of Information Technology*, 15(4): 2317–2327.

Pan, X.; Liu, M.; Zhong, F.; Yang, Y.; Zhu, S.-C.; and Wang, Y. 2022. MATE: Benchmarking multi-agent reinforcement learning in distributed target coverage control. *Advances in Neural Information Processing Systems*, 35: 27862–27879.

Rastgoftar, H. 2025. Deep and Decentralized Multi-Agent Coverage of a Target With Unknown Distribution. *IEEE Transactions on Control of Network Systems*. To appear.

Rastgoftar, H. 2026. Finite-State Decentralized Policy-Based Control With Guaranteed Ground Coverage. *arXiv preprint arXiv:2601.02109*. Accessed 2026.

Rastgoftar, H.; Atkins, E. M.; and Kolmanovsky, I. V. 2021. Scalable Vehicle Team Continuum Deformation Coordination with Eigen Decomposition. *IEEE Transactions on Automatic Control*.

Rastgoftar, H.; and Kolmanovsky, I. V. 2021. Safe affine transformation-based guidance of a large-scale multiquadcopter system. *IEEE Transactions on Control of Network Systems*, 8(2): 640–653.

Seraj, E.; Silva, A.; and Gombolay, M. 2022. Multi-UAV planning for cooperative wildfire coverage and tracking with quality-of-service guarantees. *Autonomous Agents and Multi-Agent Systems*, 36(2): 39.

Shakib, B.; Torab-Mostaedi, M.; Outokesh, M.; and Asadollahzadeh, M. 2020. Mass transfer evaluation in a multi-impeller extractor for reactive Mo (VI) extraction from aqueous Sulphate solution by utilizing coupling of acid and solvating Extractants. *Heat and Mass Transfer*, 56: 1995–2006.

Song, J.; Gu, Y.; and Kumar, E. 2023. Chest disease image classification based on spectral clustering algorithm. *Research Reports on Computer Science*, 77–90.

Stuart, A. M.; and Wolfram, M.-T. 2020. Inverse optimal transport. *SIAM Journal on Applied Mathematics*, 80(1): 599–619.

Wang, W.; Ozolek, J. A.; Slepčev, D.; Lee, A. B.; Chen, C.; and Rohde, G. K. 2010. An optimal transportation approach for nuclear structure-based pathology. *IEEE transactions on medical imaging*, 30(3): 621–631.

Zahed, M. J. H.; and Rastgoftar, H. 2025. Deep Neural Network-Based Aerial Transport in the Presence of Cooperative and Uncooperative UAS. *arXiv preprint arXiv:2512.06577*. Accessed 2025.